

involve

a journal of mathematics

Investigating cholera using an SIR model
with age-class structure and optimal control

K. Renee Fister, Holly Gaff, Elsa Schaefer,
Glenna Buford and Bryce C. Norris



Investigating cholera using an SIR model with age-class structure and optimal control

K. Renee Fister, Holly Gaff, Elsa Schaefer,
Glenna Buford and Bryce C. Norris

(Communicated by Suzanne Lenhart)

The use of systems of differential equations in mathematical modeling in conjunction with epidemiology continues to be an area of focused research. This paper briefly acquaints readers with epidemiology, cholera, and the need for effective control strategies; discusses cholera dynamics through a variation on the SIR epidemiological model in which two separate age classes exist in a population; finds the numeric value for R_0 to be approximately 1.54 using estimated parameters for Bangladesh; and employs an optimal control resulting in a suggestion that a protection control be implemented at the end of the monsoon season.

1. Definition of epidemiology and cholera

The World Health Organization defines epidemiology as: “the study of the distribution and determinants of health-related states or events (including disease), and the application of this study to the control of diseases and other health problems” [WHO 2012c]. Notice, this definition addresses two foundational questions regarding any disease. The first question is simply, “How does this disease work?” Once that question is adequately answered, epidemiologists ask the natural follow-up question, “How can we control this disease?”

Diarrheal disease is the fifth most deadly disease category in the world claiming more lives annually than HIV and the deadliest of cancers [WHO 2012d]. Cholera is a fast-acting diarrheal disease capable of causing death within hours of the onset of symptoms [WHO 2012b]. Again, we reference the expertise of the World Health Organization to provide an excellent definition for cholera:

MSC2010: 35L45, 35L50, 92D30.

Keywords: endemic cholera, SIR model, age class structure, ordinary differential equations, optimal control.

We would like to acknowledge that this research has been made possible through a collaborator grant from the National Science Foundation, DMS-0813563.

Cholera is an acute intestinal infection caused by ingestion of food or water contaminated with the bacterium *Vibrio cholerae*. It has a short incubation period, from less than one day to five days, and produces an enterotoxin that causes a copious, painless, watery diarrhoea that can quickly lead to severe dehydration and death if treatment is not promptly given. Vomiting also occurs in most patients. [WHO 2012a]

Having been in existence since the time of Christ and still having no cure, cholera is an excellent candidate for one of the longest-standing diseases in human history [Barua and Greenough 1992]. Cholera and similar diseases have been virtually eliminated in modernized nations through rigorous sanitation and waste treatment infrastructure [WHO 2012b]. Treatment of cholera continues to be challenging for those nations unable to effectively implement these more cost-prohibitive strategies.

2. Introduction to the two-compartment model

Among the most common epidemiological models is the standard SIR model, so named for the classifications within the model. S represents the susceptible class defined to be all of those people in a population that are not transmitting and have no immunity to the disease. I represents the infected class and is comprised of those who are transmitting the disease. Infecteds may or may not exhibit symptoms. R represents the recovered class of people who have some immunity to the disease. See Figure 1 for a depiction of this model.

One connection between the biological study of diseases and mathematics comes through differential equations. One may recall the foundational idea of calculus to be the derivative. Knowing about the derivative and how it relates to the original equation allows us to determine a representation of the original equation. Thus, if we can design a set of equations around the interaction of classes and how they are changing at any given time, we may use methods of solving differential equations to determine the number of individuals in each class at any given time.

In an attempt to analyze the effects of age on cholera dynamics, we begin with the two-compartment SIR model. This is a variation of the standard SIR model

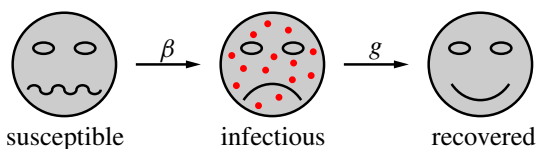


Figure 1. A pictorial representation of the standard SIR model. One may observe the nervousness of the susceptible class in anticipation of infection.

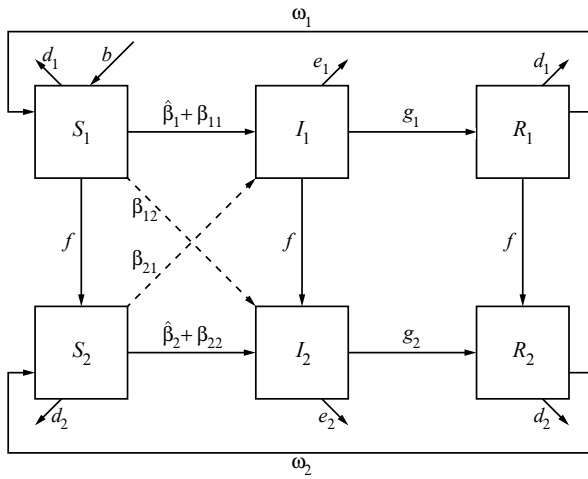


Figure 2. A pictorial representation of our two-compartment model. Dashed lines indicate an interaction between compartments, whereas solid lines indicate movement to and from compartments with $N = S_1 + S_2 + I_1 + I_2 + R_1 + R_2$.

common to biological epidemiology in which we assign classes based on age. Children under five are assigned to classes with a subscript of one. Population members at or above five years of age — henceforth referred to as matured — are assigned to the remaining classes with a subscript of two (the significance of age five is covered later in the paper). We assume that both age classes move through distinct SIR models independently except in regards to social interaction and aging. See Figure 2 for a pictorial representation of this model.

Susceptibles (denoted S_i) are defined as members of the population capable of contracting the disease (becoming infected) which implies that members of this class have no immunity to the disease. It is worth noting the underlying assumption that prior to the introduction of the disease, the entire host population is susceptible.

We define infected population members (denoted I_j) to be those capable of transmitting the disease — not necessarily those who show symptoms. Logically, these classes are assumed to be empty before the introduction of the disease.

Finally, the recovered class (denoted R_k) represents the population that has obtained, by some means, immunity to the disease. The movement of population members between these classes is discussed in the following section.

3. Two-compartment model differential equations

Our goal in studying this model is to discuss the dynamics and control of age-structured models of cholera. To this end we will translate our conceptual model from picture to ordinary differential equations as follows. A discussion of the

meaning of the terms occurs in [Section 3.1](#).

$$\frac{dS_1}{dt} = bN - \frac{\beta_{11}S_1I_1}{N} - \frac{\beta_{12}S_1I_2}{N} - \hat{\beta}_1S_1 - fS_1 - d_1S_1 + \omega_1R_1, \quad (3-1)$$

$$\frac{dS_2}{dt} = fS_1 - \frac{\beta_{21}S_2I_1}{N} - \frac{\beta_{22}S_2I_2}{N} - \hat{\beta}_2S_2 - d_2S_2 + \omega_2R_2, \quad (3-2)$$

$$\frac{dI_1}{dt} = \frac{\beta_{11}S_1I_1}{N} + \frac{\beta_{12}S_1I_2}{N} + \hat{\beta}_1S_1 - fI_1 - g_1I_1 - e_1I_1, \quad (3-3)$$

$$\frac{dI_2}{dt} = \frac{\beta_{21}S_2I_1}{N} + \frac{\beta_{22}S_2I_2}{N} + \hat{\beta}_2S_2 + fI_1 - g_2I_2 - e_2I_2, \quad (3-4)$$

$$\frac{dR_1}{dt} = g_1I_1 - fR_1 - \omega_1R_1 - d_1R_1, \quad (3-5)$$

$$\frac{dR_2}{dt} = g_2I_2 + fR_1 - \omega_2R_2 - d_2R_2, \quad (3-6)$$

subject to initial conditions $S_1(0) = S_{10}$, $S_2(0) = S_{20}$, $I_1(0) = I_{10}$, $I_2(0) = I_{20}$, $R_1(0) = R_{10}$, $R_2(0) = R_{20}$.

3.1. Equation descriptions. The equations are generally easy to generate by interpreting the pictorial model as a flow chart. As intuition would suggest, positive terms indicate entrance into a class, and negative terms indicate removal. It is worth noting that every term that enters a class must, at some point, be removed from another class (with the exception of the population growth term b). It would seem logical to assume the converse, but the introduction of death rates limits this assumption as each class has a death-rate term that does not enter any other class.

The $\beta_{ij}S_iI_j$ terms — the subscript of β is derived from the subscripts of the S and I classes respectively between whom the interaction is taking place — have a denominator of N , which is defined to be the total number of people in the system. These “mass action” (or frequency dependent) transmission terms come from the research of Keeling and Rohani [2008] and have been introduced to model the heterogeneous interaction tendencies of human populations. Every other class transfer rate is dependent solely upon the class from which it originates. Thus, every other term in the equations consists of a rate multiplied by its associated class. With this in mind, let us now consider our individual equations.

From the model, we expect that the only inputs (positive terms) for the S_1 class will come from population growth rate (represented by b) multiplied by the population size (recall that this term is defined as N) and, less intuitively, the loss of a recovered child’s immunity to cholera over the course of time shown by rate ω_1 .

Turning our attention to (3-1), we expect that some proportion (β_{1j}) of interactions of susceptible children with infecteds — two distinct terms representing interactions with both matured infecteds I_2 and children I_1 — will produce a new infected child. Data for Bangladesh, where cholera is endemic, suggests that vibrios may be

reintroduced to a system periodically by environmental factors [Ryan and Charles 2011]. To accommodate this information, an environmental forcing term ($\hat{\beta}_1$) is introduced. We also must account for a natural death rate (d_1) of children in our model population being removed from our S_1 class by inserting a term $d_1 S_1$. Lastly, we assume that children become matured at rate f , and thus move from S_1 to S_2 .

Let us discuss (3-2) by collecting the positive terms first. We assume that the S_2 class has only two inputs: one from the advancement of children to matured individuals (rate f) and the second from matured recovered losing immunity to the disease (rate ω_2). Looking at outputs, we should expect to see similar interaction terms as appeared in the dS_1/dt equation. One infection term accounts for new infections resulting from the interaction of matured individuals with children, a second term accounts for those resulting from interactions among matured individuals, and a final term models infection of matured population due to environmental factors. The introduction of a natural death rate for adults in our population (rate d_2) provides the mortality term for our equation.

When considering the infected classes, we expect to see positive terms representing interactions between susceptibles and infecteds as well as terms representing environmental factors that result in new infections. Because cholera has no direct effect on the process of aging, we still expect children to become adults in the infected classes at the same rate (f) as in the susceptible classes. A certain proportion of those infected with cholera will recover and retain some immunity to the disease (at rates g_1 and g_2) moving them out of the infected class into the recovered class. We introduce a term for the death rate of infected individuals (rates e_1 and e_2) that includes the risk of cholera-related death.

In this model, the only way in which children may enter the recovered class R_1 is to survive the disease — which we have defined to happen at rate g_1 . This is a limiting assumption that ignores the possibility of inoculation. Field research seems to indicate that surviving cholera infection does confer some degree of immunity; however, this immunity does not persist for the survivor's lifetime. For our purposes, the loss of immunity is modeled by a waning immunity rate (ω_1) that moves the population out of the recovered class back into the susceptible class. In addition, King et al. [2008] have found a variety of estimates of the time for which immunity persists.

The death rate for the recovered population is assumed to be the natural rate (d_1), and children continue to move into the matured class at the rate f . This means that the matured recovered population may be increased by either mature population members surviving the disease (rate g_2) or children surviving the disease and maturing during the period in which they have some degree of immunity (represented by the familiar age-class-advancement term f). We assume that recovered individuals die at the natural rate (d_2) and that they lose immunity and return to the susceptible population at a rate of ω_2 .

3.2. Parameter estimates. The following subsections contain a discussion of our parameter estimates for the selected population in Bangladesh. During our research, we became particularly interested in endemic cholera, and found data from Bangladesh readily available. However, it is worth noting that the appropriate selection of parameters would allow this system to model cholera for two age classes in any population.

After exploration of the Wolfram Alpha information database [2010], we concluded that a natural death rate for Bangladesh should be 0.0092 people per person per year, and the birth rate should be 0.0247 people per person per year. Because our model analyzes the system in days, it is expedient for us to ensure that the units on all of our rates are also in days. The result of these and the remaining parameter calculations may be seen in Table 1.

The dissertation work of Peng Zhong [2011] seems to indicate a relatively low death rate as compared to the rate of deaths caused by cholera — .0014 people per person per year. This estimation would include a number of control tactics actually being used in the field. As our intention is to develop a system that accurately models real-world data in Bangladesh, the use of this parameter estimate is warranted. However, we must again convert into the proper unit of measure and account for naturally occurring deaths.

The research of Harris et al. [2008] among others, [Ryan 2011; Ryan and Charles 2011], posits statistical significance of increased risk of infection for children under five. Thus, we have chosen five years as our significant age for class advancement. Calculating a rate of advancement of the first age class to the second seems to be a simple matter of arithmetic, dividing the birth rate by the number of days in five years to find an appropriate rate.

Again, Harris et al. [2008] gave us a significant clue as to what parameter values to use in modeling the interaction between infected and susceptible classes. Their conclusion was that twenty-one percent of household contacts “...develop definite *V. cholerae* infections...” and “...children 5 years of age or younger ... were 2.7 times...” as likely to develop infections as were “older individuals”. Thus, a bit of algebra gives us estimates for our interaction parameters.

The forcing term used is a randomized Heaviside function, which we sought to use to model the monsoon season in Bangladesh and east India where cholera outbreaks are common. We used Bangladesh’s monsoon data [Sack et al. 2003], and concluded that the monsoon season lasts from the beginning of June through the end of September. With this information, we “turned on” our Heaviside function on the 152nd day of the year (corresponding with June 1) and “turned off” our Heaviside function on the 254th day of the year (corresponding with September 30). During monsoon season, the Heaviside function assigns $\hat{\beta}_i$, a random proportion, for each day. This allows us to account for the randomness of nature in that the

symbol	description	rate
b	birth rate of the entire population ¹	$6.8 \times 10^{-5} \text{ day}^{-1}$
d_1	natural death rate of children ¹	$2.5 \times 10^{-5} \text{ day}^{-1}$
d_2	natural death rate of matured individuals ¹	$2.5 \times 10^{-5} \text{ day}^{-1}$
f	proportion of children maturing ²	$7.8 \times 10^{-7} \text{ day}^{-1}$
β_{11}	child infections resulting from interactions between susceptible children and infected children ²	$1.5 \times 10^{-1} \text{ day}^{-1}$
β_{12}	child infections resulting from interactions between susceptible children and matured infecteds ²	$1.5 \times 10^{-1} \text{ day}^{-1}$
β_{21}	matured infections resulting from interactions between matured susceptibles and infected children ²	$5.7 \times 10^{-2} \text{ day}^{-1}$
β_{22}	matured infections resulting from interactions between matured susceptibles and matured infecteds ²	$5.7 \times 10^{-2} \text{ day}^{-1}$
$\hat{\beta}_1$	environmental forcing term for children	Heaviside
$\hat{\beta}_2$	environmental forcing term for mature individuals	Heaviside
e_1	death rate of child-aged infected population ¹	$2.9 \times 10^{-5} \text{ day}^{-1}$
e_2	death rate of matured infected population ¹	$2.9 \times 10^{-5} \text{ day}^{-1}$
g_1	infected children to recovered children transition ^{3,4}	$6.7 \times 10^{-2} \text{ day}^{-1}$
g_2	infected adults to recovered adults transition ^{3,4}	$6.7 \times 10^{-2} \text{ day}^{-1}$
ω_1	waning immunity rate of children ⁵	$2.2 \times 10^{-3} \text{ day}^{-1}$
ω_2	waning immunity rate of matured individuals ⁵	$2.2 \times 10^{-3} \text{ day}^{-1}$

Table 1. Two-compartment parameter estimates. Key: ¹ = [Wolfram Alpha 2010]; ² = [Harris et al. 2008]; ³ = [Nelson et al. 2009]; ⁴ = [WHO 2012b]; ⁵ = [Zhong 2011].

effects of rain and floods could vary significantly day by day. It is important to note that, although the forcing terms obtain new values for each time step, they are considered constant for each time step.

Here we define

$$\hat{\beta}_i = \begin{cases} \text{rand} & \text{if } 152 \leq t \text{ mod } 365 \leq 254, \\ 0 & \text{elsewhere,} \end{cases}$$

where $i = 1, 2$ and rand is the MATLAB function reference that generates random numbers whose elements are uniformly distributed in the interval (0, 1).

As noted previously, the rate at which recovered members of the population lose immunity is difficult to accurately estimate. We elected to use estimates from [Zhong 2011] in our model; however, we wish to note that in [Nelson et al. 2009], they observe that these rates assume almost entirely asymptomatic infections within the population which is not supported by recent studies.

We determined an appropriate estimation of the length of a cholera infection to be fifteen days. As such, we are easily able to calculate the rate of recovery of the infected classes.

Table 1 contains estimates for parameters used in the two-compartment model, short descriptions of the parameters, and the source references for our estimates.

4. R_0 calculation

R_0 , or the basic reproductive ratio, is commonly defined to be the mean number of secondary cases resulting from a single primary infection within a population. This is a useful measure of the epidemicity, or speed of spread, of a disease. In calculating R_0 , we used the methods outlined by van den Driessche and Watmough [2002]. In order to carefully calculate R_0 , we recognize that if there is no disease present initially, then the population remains disease-free for all time. The $\hat{\beta}_i$ coefficients for $i = 1, 2$ cause a challenge. Therefore, we analyze the system with the $\hat{\beta}_i$ values for $i = 1, 2$ equal to zero. If the disease is spread in this case, it would also spread with nonzero $\hat{\beta}_i$ coefficients. Using this assumption within the system (3-1)–(3-6), we use the next generation matrix technique as follows.

\mathcal{F} is formed by compiling the terms that bring new infections into an infected class. For the sake of convenience and clarity, we rearranged the differential equations in such a way that the infected classes are at the top (i.e., $I_1, I_2, S_1, S_2, R_1, R_2$). This operation is permitted by common linear algebra operations; however, its application must be consistent through the calculation. The vector \mathcal{V} is constructed by compiling the additive inverse of the remaining terms such that our state equations can be determined by taking $\mathcal{F} - \mathcal{V}$.

It is important to note that only new infections are considered in \mathcal{F} . Movement between infected classes is shown in \mathcal{V} :

$$\mathcal{F} = \begin{bmatrix} \beta_{11}S_1I_1N^{-1} + \beta_{12}S_1I_2N^{-1} \\ \beta_{21}S_2I_1N^{-1} + \beta_{22}S_2I_2N^{-1} \\ 0 \\ 0 \\ 0 \\ 0 \end{bmatrix}, \quad (4-1)$$

$$\mathcal{V} = \begin{bmatrix} fI_1 + g_1I_1 + e_1I_1 \\ -fI_1 + g_2I_2 + e_2I_2 \\ -bN + \beta_{11}S_1I_1N^{-1} + \beta_{12}S_1I_2N^{-1} + \bar{\beta}_1S_1 + fS_1 + d_1S_1 - \omega_1R_1 \\ -fS_1 + \beta_{21}S_2I_1N^{-1} + \beta_{22}S_2I_2N^{-1} + \bar{\beta}_2S_2 + d_2S_2 - \omega_2R_2 \\ -g_1 + fR_1 + \omega_1R_1 + d_1R_1 \\ -g_2I_2 - fR_1 + \omega_2R_2 + d_2R_2 \end{bmatrix}. \quad (4-2)$$

We then calculate the disease-free equilibrium (henceforth DFE) — mathematically denoted \vec{x}_0 — by setting the state equations equal to zero and $I_1 = I_2 = 0 = R_1 = R_2$. This comes from the assumption that the DFE is the state of our population before the introduction of the disease. From this assumption, we get

$$\vec{x}_0 = (0, 0, S_1(0), S_2(0), 0, 0). \tag{4-3}$$

Following [van den Driessche and Watmough 2002], the square matrix F is calculated by taking the partial derivatives of \mathcal{F} with respect to I_1 and I_2 , evaluating at the DFE, and placing the resulting column vector into corresponding columns of F . Symbolically, we have

$$F = \begin{bmatrix} \frac{\partial \mathcal{F}}{\partial I_1}(\vec{x}_0) & \frac{\partial \mathcal{F}}{\partial I_2}(\vec{x}_0) \end{bmatrix} = \begin{bmatrix} \frac{\beta_{11}S_{10}}{S_{10}+S_{20}} & \frac{\beta_{12}S_{10}}{S_{10}+S_{20}} \\ \frac{\beta_{21}S_{20}}{S_{10}+S_{20}} & \frac{\beta_{22}S_{20}}{S_{10}+S_{20}} \end{bmatrix}, \tag{4-4}$$

where S_{10} and S_{20} are the initial populations of the S_1 and S_2 classes respectively. A similar process is used in calculating the square matrix V :

$$V = \begin{bmatrix} \frac{\partial \mathcal{V}}{\partial I_1}(\vec{x}_0) & \frac{\partial \mathcal{V}}{\partial I_2}(\vec{x}_0) \end{bmatrix} = \begin{bmatrix} f + g_1 + e_1 & 0 \\ -f & e_2 + g_2 \end{bmatrix} \Rightarrow V^{-1} = \frac{1}{\alpha\gamma} \begin{bmatrix} \gamma & 0 \\ f & \alpha \end{bmatrix},$$

where $\alpha = f + e_1 + g_1$ and $\gamma = e_2 + g_2$.

Generally, $R_0 \equiv \rho(FV^{-1})$, where ρ is the spectral radius, or maximum magnitude of the spectrum of a square matrix [van den Driessche and Watmough 2002]. Thus, R_0 is calculated by finding the spectrum of FV^{-1} , namely $\text{eig}(FV^{-1})$, and determining the largest value in terms of absolute value. For our model,

$$\begin{aligned} FV^{-1} &= \frac{1}{\alpha\gamma(S_{10}+S_{20})} \begin{bmatrix} \beta_{11}S_{10} & \beta_{12}S_{10} \\ \beta_{21}S_{20} & \beta_{22}S_{20} \end{bmatrix} \begin{bmatrix} \gamma & 0 \\ f & \alpha \end{bmatrix} \\ &= \frac{1}{\alpha\gamma(S_{10}+S_{20})} \begin{bmatrix} \beta_{11}S_{10}\gamma + \beta_{12}S_{10}f & \beta_{12}S_{10}\alpha \\ \beta_{21}S_{20}\gamma + \beta_{22}S_{20}f & \beta_{22}S_{20}\alpha \end{bmatrix}. \end{aligned}$$

We consider

$$\lambda I - FV^{-1} = \begin{bmatrix} \lambda - \frac{\beta_{11}S_{10}\gamma + \beta_{12}S_{10}f}{\alpha\gamma(S_{10}+S_{20})} & -\frac{\beta_{12}S_{10}\alpha}{\alpha\gamma(S_{10}+S_{20})} \\ -\frac{\beta_{21}S_{20}\gamma + \beta_{22}S_{20}f}{\alpha\gamma(S_{10}+S_{20})} & \lambda - \frac{\beta_{22}S_{20}\alpha}{\alpha\gamma(S_{10}+S_{20})} \end{bmatrix}.$$

We find the determinant of $\lambda I - FV^{-1}$ and obtain

$$0 = \lambda^2 - \lambda \left(\frac{\beta_{11}S_{10}\gamma + \beta_{12}S_{10}f + \beta_{22}S_{20}\alpha}{\alpha\gamma(S_{10} + S_{20})} \right) + \frac{\beta_{22}S_{20}\alpha(\beta_{11}S_{10}\gamma + \beta_{12}S_{10}f) - \beta_{12}S_{10}\alpha(\beta_{21}S_{20}\gamma + \beta_{22}S_{20}f)}{(\alpha\gamma(S_{10} + S_{20}))^2},$$

$$0 = (\alpha\gamma(S_{10} + S_{20}))^2\lambda^2 - \lambda(\alpha\gamma(S_{10} + S_{20}))(\beta_{11}S_{10}\gamma + \beta_{12}S_{10}f + \beta_{22}S_{20}\alpha) + \alpha\gamma S_{10}S_{20}(\beta_{22}\beta_{11} - \beta_{12}\beta_{21}).$$

Let

$$\begin{aligned}\omega &= \alpha\gamma(S_{10} + S_{20}), \\ \eta &= \beta_{11}S_{10}\gamma + \beta_{12}S_{10}f + \beta_{22}S_{20}\alpha, \\ \psi &= \alpha\gamma S_{10}S_{20}(\beta_{11}\beta_{22} - \beta_{12}\beta_{21}).\end{aligned}$$

Then we have

$$0 = \omega^2\lambda^2 - \omega\eta\lambda + \psi \quad \text{or} \quad \lambda = \frac{\eta \pm \sqrt{\eta^2 - 4\psi}}{2\omega}.$$

Here, our parameters allow some useful simplification. Because $\beta_{11} = \beta_{12}$ and $\beta_{21} = \beta_{22}$, we can say $\psi = \alpha\gamma S_{10}S_{20}(\beta_{11}\beta_{22} - \beta_{12}\beta_{21}) = 0$. This gives us an abbreviated representation of our basic reproductive ratio,

$$\lambda = 0 \quad \text{or} \quad \lambda = \frac{\eta}{\omega}.$$

We are looking for the largest absolute value; therefore,

$$R_0 \equiv \frac{\beta_{11}S_{10}\gamma + \beta_{12}S_{10}f + \beta_{22}S_{20}\alpha}{\alpha\gamma(S_{10} + S_{20})}. \quad (4-5)$$

From the general equation for R_0 and the estimates listed previously, we find the numeric value of R_0 to be approximately 1.54. Since the R_0 value is greater than 1, the disease spreads. Consequently, with the disease spreading in this case, it would also spread with nonzero $\hat{\beta}_i$ for $i = 1, 2$. These coefficients do have an impact on the behavior of the model denoted in the graphics. With this R_0 value, this indicates that each primary cholera infection introduces the disease to a portion of the remaining susceptible population. In consideration of this fact, we employed a control discussed in [Section 6](#).

5. Graphics with environmental forcing term

From the graph presented in [Figure 3](#), we can see the disease-free equilibrium, or DFE, for our model is followed by a dramatic decrease in the susceptible population and a corresponding increase in the infected population (this may be clearer in [Figure 4](#)). The infected population quickly dwindles giving rise to a recovered population with some immunity. Perhaps unexpectedly, we see a

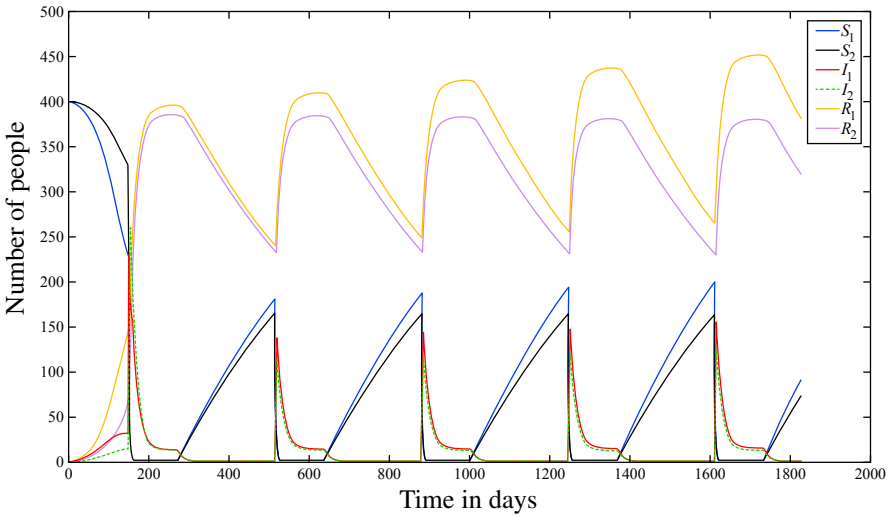


Figure 3. This represents a simulation over five years with initial data $S_1(0) = S_2(0) = 400$, $I_1(0) = I_2(0) = 1$ and $R_1(0) = R_2(0) = 0$.

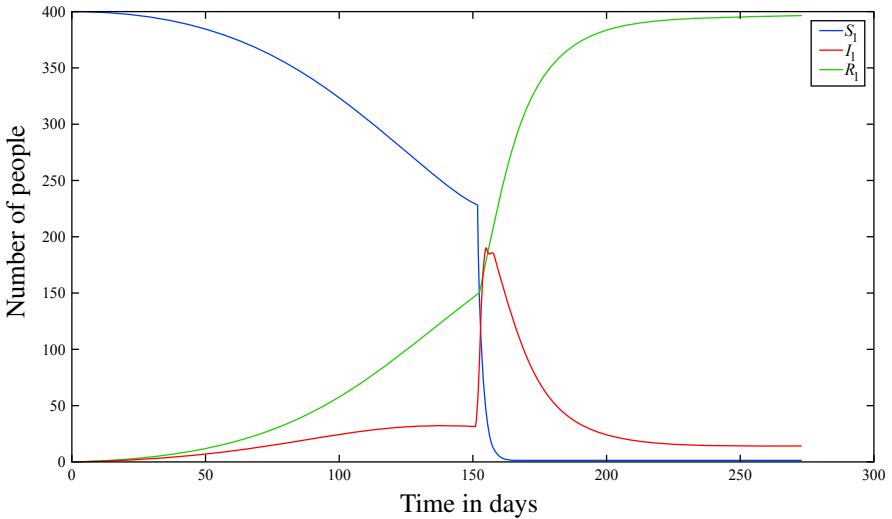


Figure 4. For the sake of clarity, this is the first 9 months of the previous simulation for children in [Figure 3](#).

cyclical pattern representing seasonal spikes in infecteds and subsequent increases in recovered individuals. This is a result of the environmental forcing terms, $\hat{\beta}_i$, which were chosen to display the effects of the Bangladeshi monsoon season on cholera dynamics.

Notice, population growth still occurs over the course of time. Since this model does not assume a closed population, we would expect population growth to be a

function of the country chosen for analysis. This conclusion seems to be in line with demographic data that indicates continued population growth despite the existence of endemic cholera in Bangladesh.

6. Optimal control

Before we consider control of the disease, we must establish the kind of control we will use. This selection has significant effect on the derivation of our new differential equations (those that include the dynamics of the control) and every subsequent step in the process of optimization. For the sake of this paper, we consider the effects of what may be called a protection control in which we limit the interaction of susceptible children with both infected classes. Our optimization process is an application addressed in the work of Lenhart and Workman [2007].

For this model we are interested in the effect of a simple control, one in which we limit the interactions of susceptible children. Symbolically, this is shown by inserting the control $(1 - u(t))$ as a coefficient of the interaction terms $\beta_{11}S_1I_1/N$ and $\beta_{12}S_1I_2/N$. That is, the control allows only part of the I_1 and I_2 classes to interact with the S_1 class. Our system of differential equations becomes

$$\frac{dS_1}{dt} = bN - \frac{(1-u)\beta_{11}S_1I_1}{N} - \frac{(1-u)\beta_{12}S_1I_2}{N} - \hat{\beta}_1S_1 - fS_1 - d_1S_1 + \omega_1R_1, \quad (6-1)$$

$$\frac{dS_2}{dt} = fS_1 - \frac{\beta_{21}S_2I_1}{N} - \hat{\beta}_2S_2 - \frac{\beta_{22}S_2I_2}{N} - d_2S_2 + \omega_2R_2, \quad (6-2)$$

$$\frac{dI_1}{dt} = \frac{(1-u)\beta_{11}S_1I_1}{N} + \frac{(1-u)\beta_{12}S_1I_2}{N} + \hat{\beta}_1S_1 - fI_1 - g_1I_1 - e_1I_1, \quad (6-3)$$

$$\frac{dI_2}{dt} = \frac{\beta_{21}S_2I_1}{N} + \frac{\beta_{22}S_2I_2}{N} + \hat{\beta}_2S_2 + fI_1 - g_2I_2 - e_2I_2, \quad (6-4)$$

$$\frac{dR_1}{dt} = g_1I_1 - fR_1 - \omega_1R_1 - d_1R_1, \quad (6-5)$$

$$\frac{dR_2}{dt} = g_2I_2 + fR_1 - \omega_2R_2 - d_2R_2, \quad (6-6)$$

subject to initial conditions $S_1(0) = S_{10}$, $S_2(0) = S_{20}$, $I_1(0) = I_{10}$, $I_2(0) = I_{20}$, $R_1(0) = R_{10}$, $R_2(0) = R_{20}$.

We wish to minimize an objective functional that represents the members of each infected class and the cost of control implementation. Perhaps put more simply, we minimize the numbers of infected children and mature adults as well as the cost of the protection control. Having a goal and method in mind, we may write

$$J(u) = \int_0^T (AI_1(t) + BI_2(t) + Cu^2(t)) dt. \quad (6-7)$$

Note that if the protection control is at 0, then the cost to the population is the least in the objective functional. If the control $u(t)$ is low, then this means a small impact on transmission. Hence, this represents a small cost to the system.

We must define our control set U , which is the set of all possible control outcomes. This set is restricted to measurable functions and must be bounded. Thus,

$$U = \{u(t) \text{ measurable} \mid 0 \leq u(t) \leq u_{\max}\}. \tag{6-8}$$

In consideration of our goal, we will attempt to minimize $J(u)$ over the class of controls U subject to equations (6-1)–(6-6).

By determining the Hamiltonian for our system, we are able to determine the necessary conditions for optimality and transversality [Lenhart and Workman 2007]. This also allows us to determine the form of the adjoint equations by taking the negative derivative of the Hamiltonian with respect to each of the state variables. The Hamiltonian is

$$\begin{aligned} H = & AI_1(t) + BI_2(t) + Cu^2(t) \\ & + \lambda_{S_1} \left(bN - \frac{(1-u)\beta_{11}S_1I_1}{N} - \frac{(1-u)\beta_{12}S_1I_2}{N} - fS_1 - d_1S_1 + \omega_1R_1 - \hat{\beta}_1S_1 \right) \\ & + \lambda_{S_2} \left(fS_1 - \frac{\beta_{21}S_2I_1}{N} - \frac{\beta_{22}S_2I_2}{N} - d_2S_2 + \omega_2R_2 - \hat{\beta}_2S_2 \right) \\ & + \lambda_{I_1} \left(\frac{(1-u)\beta_{11}S_1I_1}{N} + \frac{(1-u)\beta_{12}S_1I_2}{N} - fI_1 - g_1I_1 - e_1I_1 + \hat{\beta}_1S_1 \right) \\ & + \lambda_{I_2} \left(\frac{\beta_{21}S_2I_1}{N} + \frac{\beta_{22}S_2I_2}{N} + fI_1 - g_2I_2 - e_2I_2 + \hat{\beta}_2S_2 \right) \\ & + \lambda_{R_1}(g_1I_1 - fR_1 - \omega_1R_1 - d_1R_1) \\ & + \lambda_{R_2}(g_2I_2 + fR_1 - \omega_2R_2 - d_2R_2). \end{aligned} \tag{6-9}$$

Because the state system is bounded, the work of Fleming and Rishel [1975] allows us to obtain the existence of an optimal control for our problem. Moreover, we can formulate the adjoint equations and the optimal control representation associated with the minimization of $J(u)$ subject to equations (6-1)–(6-6). We state the following theorem to do so and reference Lenhart and Workman [2007] for the details of the complementary proof.

Theorem. *Given an optimal control $u^* \in U$ and corresponding states*

$$(S_1^*, S_2^*, I_1^*, I_2^*, R_1^*, R_2^*),$$

there exist adjoint functions $(\lambda_{S_1}, \lambda_{S_2}, \lambda_{I_1}, \lambda_{I_2}, \lambda_{R_1}, \lambda_{R_2})$ satisfying

$$\begin{aligned}
\frac{d\lambda_{S_1}}{dt} = & -\lambda_{S_1} \left(b - f - d_1 + (1-u) \left(\frac{\beta_{11}S_1I_1}{N^2} - \frac{\beta_{11}I_1}{N} + \frac{\beta_{12}S_1I_2}{N^2} - \frac{\beta_{12}I_1}{N} \right) - \hat{\beta}_1 \right) \\
& -\lambda_{S_2} \left(f + \frac{\beta_{21}S_2I_1}{N^2} + \frac{\beta_{22}S_2I_2}{N^2} \right) \\
& -\lambda_{I_1} \left(-\frac{(1-u)\beta_{11}S_1I_1}{N^2} + \frac{(1-u)\beta_{11}I_1}{N} - \frac{(1-u)\beta_{12}S_1I_2}{N^2} \right. \\
& \qquad \qquad \qquad \left. + \frac{(1-u)\beta_{12}I_1}{N} + \hat{\beta}_1 \right) \\
& -\lambda_{I_2} \left(-\frac{\beta_{21}S_2I_1}{N^2} - \frac{\beta_{22}S_2I_2}{N^2} \right), \tag{6-10}
\end{aligned}$$

$$\begin{aligned}
\frac{d\lambda_{S_2}}{dt} = & -\lambda_{S_1} \left(b + \frac{(1-u)\beta_{11}S_1I_1}{N^2} + \frac{(1-u)\beta_{12}S_1I_2}{N^2} \right) \\
& -\lambda_{S_2} \left(-d_2 + \frac{\beta_{21}S_2I_1}{N^2} - \frac{\beta_{21}I_1}{N} + \frac{\beta_{22}S_2I_2}{N^2} - \frac{\beta_{22}I_2}{N} - \hat{\beta}_2 \right) \\
& -\lambda_{I_1} \left(-\frac{(1-u)\beta_{11}S_1I_1}{N^2} - \frac{(1-u)\beta_{12}S_1I_2}{N^2} \right) \\
& -\lambda_{I_2} \left(-\frac{\beta_{21}S_2I_1}{N^2} + \frac{\beta_{21}I_1}{N} - \frac{\beta_{22}S_2I_2}{N^2} + \frac{\beta_{22}I_2}{N} + \hat{\beta}_2 \right), \tag{6-11}
\end{aligned}$$

$$\begin{aligned}
\frac{d\lambda_{I_1}}{dt} = & -\lambda_{S_1} \left(b + \frac{(1-u)\beta_{11}S_1I_1}{N^2} - \frac{(1-u)\beta_{11}S_1}{N} + \frac{(1-u)\beta_{12}S_1I_2}{N^2} \right) \\
& -\lambda_{S_2} \left(\frac{\beta_{21}S_2I_1}{N^2} - \frac{\beta_{21}S_2}{N} + \frac{\beta_{22}S_2I_2}{N^2} \right) \\
& -\lambda_{I_1} \left(-f - e_1 - g_1 - \frac{(1-u)\beta_{11}S_1I_1}{N^2} + \frac{(1-u)\beta_{11}S_1}{N} - \frac{(1-u)\beta_{12}S_1I_2}{N^2} \right) \\
& -\lambda_{I_2} \left(f - \frac{\beta_{21}S_2I_1}{N^2} + \frac{\beta_{21}S_2}{N} - \frac{\beta_{22}S_2I_2}{N^2} \right) - \lambda_{R_1} g_1, \tag{6-12}
\end{aligned}$$

$$\begin{aligned}
\frac{d\lambda_{I_2}}{dt} = & -\lambda_{S_1} \left(b + \frac{(1-u)\beta_{11}S_1I_1}{N^2} + \frac{(1-u)\beta_{12}S_1I_2}{N^2} - \frac{(1-u)\beta_{12}S_1}{N} \right) \\
& -\lambda_{S_2} \left(\frac{\beta_{21}S_2I_1}{N^2} + \frac{\beta_{22}S_2I_2}{N^2} - \frac{\beta_{22}S_2}{N} \right) \\
& -\lambda_{I_1} \left(-\frac{(1-u)\beta_{11}S_1I_1}{N^2} - \frac{(1-u)\beta_{12}S_1I_2}{N^2} + \frac{(1-u)\beta_{12}S_1}{N} \right) \\
& -\lambda_{I_2} \left(-e_2 - g_2 - \frac{\beta_{21}S_2I_1}{N^2} - \frac{\beta_{22}S_2I_2}{N^2} + \frac{\beta_{22}S_2}{N} \right) - \lambda_{R_2} g_2, \tag{6-13}
\end{aligned}$$

$$\begin{aligned}
 \frac{d\lambda_{R_1}}{dt} = & -\lambda_{S_1} \left(b + \frac{(1-u)\beta_{11}S_1I_1}{N^2} + \frac{(1-u)\beta_{12}S_1I_2}{N^2} + \omega_1 \right) \\
 & -\lambda_{S_2} \left(\frac{\beta_{21}S_2I_1}{N^2} + \frac{\beta_{22}S_2I_2}{N^2} \right) \\
 & -\lambda_{I_1} \left(-\frac{(1-u)\beta_{11}S_1I_1}{N^2} - \frac{(1-u)\beta_{12}S_1I_2}{N^2} \right) \\
 & -\lambda_{I_2} \left(-\frac{\beta_{21}S_2I_1}{N^2} - \frac{\beta_{22}S_2I_2}{N^2} \right) - \lambda_{R_1}(-f-d_1-\omega_1) - f\lambda_{R_2}, \quad (6-14)
 \end{aligned}$$

$$\begin{aligned}
 \frac{d\lambda_{R_2}}{dt} = & -\lambda_{S_1} \left(b + \frac{(1-u)\beta_{11}S_1I_1}{N^2} + \frac{(1-u)\beta_{12}S_1I_2}{N^2} \right) \\
 & -\lambda_{S_2} \left(\frac{\beta_{21}S_2I_1}{N^2} + \frac{\beta_{22}S_2I_2}{N^2} + \omega_2 \right) - \lambda_{I_1} \left(-\frac{(1-u)\beta_{11}S_1I_1}{N^2} - \frac{(1-u)\beta_{12}S_1I_2}{N^2} \right) \\
 & -\lambda_{I_2} \left(-\frac{\beta_{21}S_2I_1}{N^2} - \frac{\beta_{22}S_2I_2}{N^2} \right) - \lambda_{R_2}(-d_2-\omega_2), \quad (6-15)
 \end{aligned}$$

with transversality conditions

$$\lambda_{S_1}(T) = \lambda_{S_2}(T) = \lambda_{I_1}(T) = \lambda_{I_2}(T) = \lambda_{R_1}(T) = \lambda_{R_2}(T) = 0,$$

and the optimal control is characterized by

$$u^* = \min \left(u_{\max}, \max \left(0, \frac{1}{2NC} (\lambda_{I_1} - \lambda_{S_1}) (\beta_{11}S_1I_1 + \beta_{12}S_1I_2) \right) \right).$$

6.1. Discussion of control and infected classes graphics. In an attempt to see the effects of various weights on our optimal control, we ran the model with A , B , C at various orders of magnitude. Also, due to possible imperfections of human protection implementation, we tested various control levels ranging from 0.1 to 0.9. This was achieved reasonably quickly since our MATLAB code allows the bounds on the control to be specified as an input. Each of these maximum control variations displayed structurally similar results. It is worth noting that for the sake of clarity, Figures 5–7 have the control weights set to $A = 1$, $B = 1$, $C = 10$, where the cost of the control receives ten times as much emphasis.

For a time span of four years (see Figure 5), we see that our treatment should start with maximum implementation decreasing around the start of the first monsoon season. Control potency decreases dramatically through the two-hundred day mark and spikes again around the same time that we would expect the monsoon season to return. This pattern seems to be repeated with milder and shorter implementation through the remainder of the treatment period. The resulting effects on the infected classes are shown in Figures 6 and 7 and are discussed below.

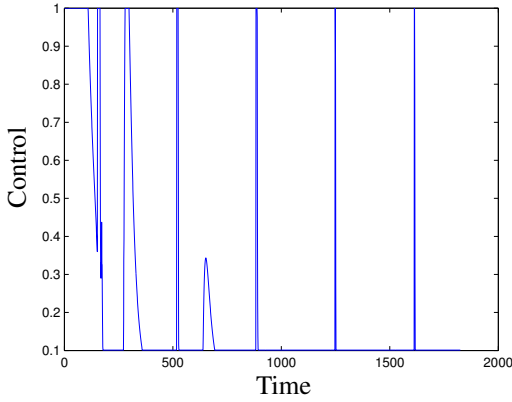


Figure 5. Our model with a forcing term and control implemented; this simulation covers a time span of 4 years with $S_1(0) = S_2(0) = 400$, $I_1(0) = I_2(0) = 1$ and $R_1(0) = R_2(0) = 0$.

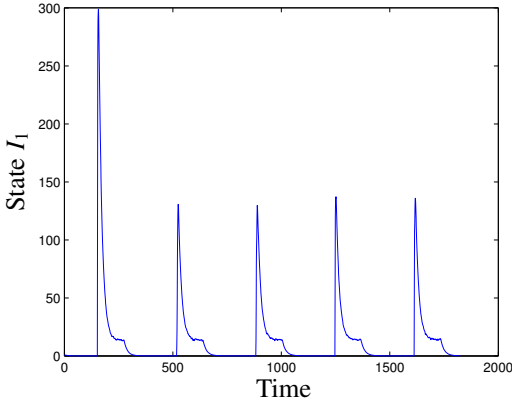


Figure 6. The effects of a five-year control on the I_1 class.

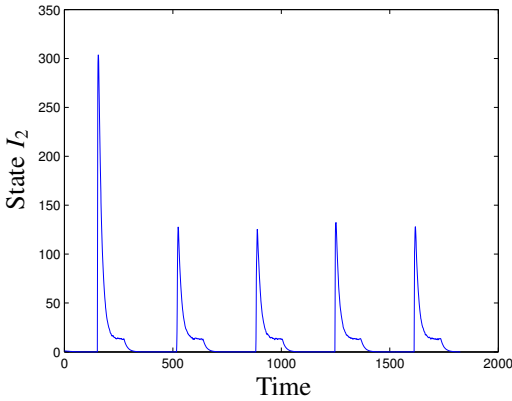


Figure 7. The effects of a five-year control on the I_2 class.

Toward the end of the first monsoon season, the model indicates that the protection control be implemented at approximately one-third efficacy. This increased protection control at the end of (or immediately following) the monsoon season, reflects data from Sack et al. [2003] which says the highest correlation seen between monsoon data and cholera outbreaks is a spike in outbreaks at the very end, immediately following the monsoon season.

In each infected class, we see a spike of infecteds at the beginning of the first monsoon season and decreasing immediately following. Notice that both classes continue to see yearly spikes, but the maximum number of infected individuals stabilizes and is limited to about 150 people per year.

7. Conclusions

Based on this specific model, it would seem advantageous to extend a protection control at the inception of each monsoon season. This would minimize the portion of the population in the infected classes over time. Additionally, it has the potential to be very cost-effective and practical. Lengthy protections would only be necessary the first year of the treatment process and this model could allow governments to schedule national protection or isolation days in advance, thus increasing the possibility of widespread compliance. One interesting insight offered by our data follows from the small increase in control around the end of the first monsoon season. It would seem that a small increase in protection control the first year is enough to disrupt the cycle of sickness and immunity loss in future years.

The results of our optimal control could have implications for consideration in future policy decisions in Bangladesh. With regard to the general strategy of analyzing treatments using nonhomogeneous age classes, benefits may be recognized through practical consideration. Social dynamics often vary greatly by age causing incongruencies between the assumptions of social homogeneity common to many epidemiological models and the actual practices of most cultures. For this reason, this work may offer clearer and more functional results for policy implementation.

References

- [Barua and Greenough 1992] D. Barua and W. B. Greenough, III (editors), *Cholera*, Springer, New York, 1992.
- [van den Driessche and Watmough 2002] P. van den Driessche and J. Watmough, “Reproduction numbers and sub-threshold endemic equilibria for compartmental models of disease transmission”, *Math. Biosci.* **180** (2002), 29–48. [MR 2003m:92071](#) [Zbl 1015.92036](#)
- [Fleming and Rishel 1975] W. H. Fleming and R. W. Rishel, *Deterministic and stochastic optimal control*, Applications of Mathematics **1**, Springer, New York, 1975. [MR 56 #13016](#) [Zbl 0323.49001](#)
- [Harris et al. 2008] J. B. Harris, R. C. LaRocque, F. Chowdhury, A. I. Khan, T. Logvinenko, A. S. G. Faruque, E. T. Ryan, F. Qadri, and S. B. Calderwood, “Susceptibility to *Vibrio cholerae* infection in

- a cohort of household contacts of patients with cholera in Bangladesh”, *PLoS Negl. Trop. Dis.* **2**:4 (2008), e221.
- [Keeling and Rohani 2008] M. J. Keeling and P. Rohani, *Modeling infectious diseases in humans and animals*, Princeton University Press, 2008. MR 2008f:92068 Zbl 1279.92038
- [King et al. 2008] A. A. King, E. L. Ionides, M. Pascual, and M. J. Bouma, “Inapparent infections and cholera dynamics”, *Nature* **454**:7206 (2008), 877–881.
- [Lenhart and Workman 2007] S. Lenhart and J. T. Workman, *Optimal control applied to biological models*, Chapman & Hall/CRC, Boca Raton, FL, 2007. MR 2008f:49001 Zbl 1291.92010
- [Nelson et al. 2009] E. J. Nelson, J. B. Harris, J. G. Morris, Jr., S. B. Calderwood, and A. Camilli, “Cholera transmission: the host, pathogen and bacteriophage dynamic”, *Nat. Rev. Microbiol.* **7** (2009), 693–702.
- [Ryan 2011] E. T. Ryan, “The cholera pandemic, still with us after half a century”, *PLoS Negl. Trop. Dis.* **5**:1 (2011), e1003.
- [Ryan and Charles 2011] E. T. Ryan and R. C. Charles, “Cholera in the 21st century”, *Current Opinion in Infectious Diseases* **24**:5 (2011), 472–477.
- [Sack et al. 2003] R. B. Sack, A. K. Siddique, J. Ira, M. Longini, A. Nizham, M. Yunus, M. S. Islam, J. J. G. Morris, A. Ali, A. Huq, G. B. Nair, F. Qadri, S. M. Faruque, D. A. Sack, and R. R. Colwell, “A 4-year study of the epidemiology of *Vibrio cholerae* in four rural areas of Bangladesh”, *J. Infect. Dis.* **287**:1 (2003), 96–101.
- [WHO 2012a] World Health Organization, “Cholera”, website, 2012, <http://www.who.int/topics/cholera/en/>.
- [WHO 2012b] World Health Organization, “Cholera fact sheet”, website, 2012, <http://www.who.int/mediacentre/factsheets/fs107/en/index.html>.
- [WHO 2012c] World Health Organization, “Epidemiology”, website, 2012, <http://www.who.int/topics/epidemiology/en/>.
- [WHO 2012d] World Health Organization, “The top 10 causes of death”, website, 2012, <http://www.who.int/mediacentre/factsheets/fs310/en/index.html>.
- [Wolfram Alpha 2010] Wolfram Alpha LLC, “Bangladesh annual births”, website, 2010, <http://www.wolframalpha.com/input/?i=bangladesh+births>.
- [Zhong 2011] P. Zhong, *Optimal Theory applied to integrodifference equation models in a cholera differential equation model*, Ph.D. thesis, University of Tennessee, 2011, http://trace.tennessee.edu/cgi/viewcontent.cgi?article=2287&context=utk_graddiss.

Received: 2014-01-07

Revised: 2014-12-07

Accepted: 2014-12-27

renee.fister@murraystate.edu

Department of Mathematics and Statistics,
Murray State University, Murray, KY 42071, United States

hgaff@odu.edu

Department of Biological Sciences, Old Dominion University,
Norfolk, VA 23529, United States

elsa.schaefer@marymount.edu

Department of Mathematics, Marymount University,
Arlington, VA 22207, United States

glenna.buford@wooga.com

Engineer, Wooga GmbH, Berlin, Germany

bryce.norris@gmail.com

Department of Mathematics and Statistics,
Murray State University, Murray, KY 42071, United States

MANAGING EDITOR

Kenneth S. Berenhaut, Wake Forest University, USA, berenhks@wfu.edu

BOARD OF EDITORS

Colin Adams	Williams College, USA colin.c.adams@williams.edu	David Larson	Texas A&M University, USA larson@math.tamu.edu
John V. Baxley	Wake Forest University, NC, USA baxley@wfu.edu	Suzanne Lenhart	University of Tennessee, USA lenhart@math.utk.edu
Arthur T. Benjamin	Harvey Mudd College, USA benjamin@hmc.edu	Chi-Kwong Li	College of William and Mary, USA ckli@math.wm.edu
Martin Bohner	Missouri U of Science and Technology, USA bohner@mst.edu	Robert B. Lund	Clemson University, USA lund@clemson.edu
Nigel Boston	University of Wisconsin, USA boston@math.wisc.edu	Gaven J. Martin	Massey University, New Zealand g.j.martin@massey.ac.nz
Amarjit S. Budhiraja	U of North Carolina, Chapel Hill, USA budhiraj@email.unc.edu	Mary Meyer	Colorado State University, USA meyer@stat.colostate.edu
Pietro Cerone	La Trobe University, Australia P.Cerone@latrobe.edu.au	Emil Minchev	Ruse, Bulgaria eminchev@hotmail.com
Scott Chapman	Sam Houston State University, USA scott.chapman@shsu.edu	Frank Morgan	Williams College, USA frank.morgan@williams.edu
Joshua N. Cooper	University of South Carolina, USA cooper@math.sc.edu	Mohammad Sal Moselehian	Ferdowsi University of Mashhad, Iran ferdowsi.um.ac.ir
Jem N. Corcoran	University of Colorado, USA corcoran@colorado.edu	Zuhair Nashed	University of Central Florida, USA znashed@mail.ucf.edu
Toka Diagana	Howard University, USA tdiagana@howard.edu	Ken Ono	Emory University, USA ono@mathcs.emory.edu
Michael Dorff	Brigham Young University, USA mdorff@math.byu.edu	Timothy E. O'Brien	Loyola University Chicago, USA tbriell@luc.edu
Sever S. Dragomir	Victoria University, Australia sever@matilda.vu.edu.au	Joseph O'Rourke	Smith College, USA orourke@cs.smith.edu
Behrouz Emamizadeh	The Petroleum Institute, UAE bemamizadeh@pi.ac.ae	Yuval Peres	Microsoft Research, USA peres@microsoft.com
Joel Foisy	SUNY Potsdam foisyjs@potsdam.edu	Y.-F. S. Pétermann	Université de Genève, Switzerland petermann@math.unige.ch
Errin W. Fulp	Wake Forest University, USA fulp@wfu.edu	Robert J. Plemmons	Wake Forest University, USA rplemmons@wfu.edu
Joseph Gallian	University of Minnesota Duluth, USA kgallian@d.umn.edu	Carl B. Pomerance	Dartmouth College, USA carl.pomerance@dartmouth.edu
Stephan R. Garcia	Pomona College, USA stephan.garcia@pomona.edu	Vadim Pomomarenko	San Diego State University, USA vadim@sciences.sdsu.edu
Anant Godbole	East Tennessee State University, USA godbole@etsu.edu	Bjorn Poonen	UC Berkeley, USA poonen@math.berkeley.edu
Ron Gould	Emory University, USA rg@mathcs.emory.edu	James Propp	U Mass Lowell, USA jpropp@cs.uml.edu
Andrew Granville	Université Montréal, Canada andrew@dms.umontreal.ca	József H. Przytycki	George Washington University, USA przytyck@gwu.edu
Jerrold Griggs	University of South Carolina, USA griggs@math.sc.edu	Richard Rebarber	University of Nebraska, USA rrebarbe@math.unl.edu
Sat Gupta	U of North Carolina, Greensboro, USA sgupta@uncg.edu	Robert W. Robinson	University of Georgia, USA rwr@cs.uga.edu
Jim Haglund	University of Pennsylvania, USA jhaglund@math.upenn.edu	Filip Saidak	U of North Carolina, Greensboro, USA f_saidak@uncg.edu
Johnny Henderson	Baylor University, USA johnny_henderson@baylor.edu	James A. Sellers	Penn State University, USA sellersj@math.psu.edu
Jim Hoste	Pitzer College jhoste@pitzer.edu	Andrew J. Sterge	Honorary Editor andy@ajsterge.com
Natalia Hritonenko	Prairie View A&M University, USA nhritonenko@pvamu.edu	Ann Trenk	Wellesley College, USA atrenk@wellesley.edu
Glenn H. Hurlbert	Arizona State University, USA hurlbert@asu.edu	Ravi Vakil	Stanford University, USA vakil@math.stanford.edu
Charles R. Johnson	College of William and Mary, USA crjohnso@math.wm.edu	Antonia Vecchio	Consiglio Nazionale delle Ricerche, Italy antonia.vecchio@cnr.it
K. B. Kulasekera	Clemson University, USA kk@ces.clemson.edu	Ram U. Verma	University of Toledo, USA verma99@msn.com
Gerry Ladas	University of Rhode Island, USA gladas@math.uri.edu	John C. Wierman	Johns Hopkins University, USA wierman@jhu.edu
		Michael E. Zieve	University of Michigan, USA zieve@umich.edu

PRODUCTION

Silvio Levy, Scientific Editor


Cover: Alex Scorpan

See inside back cover or msp.org/involve for submission instructions. The subscription price for 2016 is US \$160/year for the electronic version, and \$215/year (+\$35, if shipping outside the US) for print and electronic. Subscriptions, requests for back issues from the last three years and changes of subscribers address should be sent to MSP.

Involve (ISSN 1944-4184 electronic, 1944-4176 printed) at Mathematical Sciences Publishers, 798 Evans Hall #3840, c/o University of California, Berkeley, CA 94720-3840, is published continuously online. Periodical rate postage paid at Berkeley, CA 94704, and additional mailing offices.

Involve peer review and production are managed by EditFlow® from Mathematical Sciences Publishers.

PUBLISHED BY

 **mathematical sciences publishers**
nonprofit scientific publishing

<http://msp.org/>

© 2016 Mathematical Sciences Publishers

involve

2016

vol. 9

no. 1

Using ciliate operations to construct chromosome phylogenies	1
JACOB L. HERLIN, ANNA NELSON AND MARION SCHEEPERS	
On the distribution of the greatest common divisor of Gaussian integers	27
TAI-DANAE BRADLEY, YIN CHOI CHENG AND YAN FEI LUO	
Proving the pressing game conjecture on linear graphs	41
ELIOT BIXBY, TOBY FLINT AND ISTVÁN MIKLÓS	
Polygonal bicycle paths and the Darboux transformation	57
IAN ALEVY AND EMMANUEL TSUKERMAN	
Local well-posedness of a nonlocal Burgers' equation	67
SAM GOODCHILD AND HANG YANG	
Investigating cholera using an SIR model with age-class structure and optimal control	83
K. RENEE FISTER, HOLLY GAFF, ELSA SCHAEFER, GLENNA BUFORD AND BRYCE C. NORRIS	
Completions of reduced local rings with prescribed minimal prime ideals	101
SUSAN LOEPP AND BYRON PERPETUA	
Global regularity of chemotaxis equations with advection	119
SAAD KHAN, JAY JOHNSON, ELLIOT CARTEE AND YAO YAO	
On the ribbon graphs of links in real projective space	133
IAIN MOFFATT AND JOHANNA STRÖMBERG	
Depths and Stanley depths of path ideals of spines	155
DANIEL CAMPOS, RYAN GUNDERSON, SUSAN MOREY, CHELSEY PAULSEN AND THOMAS POLSTRA	
Combinatorics of linked systems of quartet trees	171
EMILI MOAN AND JOSEPH RUSINKO	